High CO_2 Primes Plant Biotic Stress Defences through Redox-Linked Pathways[1][OPEN]

Amna Mhamdi[2] and Graham Noctor*

Institute of Plant Sciences Paris Saclay, Université Paris-Sud, Centre National de la Recherche Scientifique, Institut National de la Recherche Agronomique, Université Evry, Paris Diderot, Sorbonne Paris-Cité, Université Paris-Saclay, 91405 Orsay, France

ORCID IDs: 0000-0001-9959-1362 (A.M.); 0000-0003-1980-4554 (G.N.).

Industrial activities have caused tropospheric CO_2 concentrations to increase over the last two centuries, a trend that is predicted to continue for at least the next several decades. Here, we report that growth of plants in a CO_2-enriched environment activates responses that are central to defense against pathogenic attack. Salicylic acid accumulation was triggered by high-growth CO_2 in Arabidopsis (*Arabidopsis thaliana*) and other plants such as bean (*Phaseolus vulgaris*). A detailed analysis in Arabidopsis revealed that elevated CO_2 primes multiple defense pathways, leading to increased resistance to bacterial and fungal challenge. Analysis of gene-specific mutants provided no evidence that activation of plant defense pathways by high CO_2 was caused by stomatal closure. Rather, the activation is partly linked to metabolic effects involving redox signaling. In support of this, genetic modification of redox components (glutathione contents and NADPH-generating enzymes) prevents full priming of the salicylic acid pathway and associated resistance by high CO_2. The data point to a particularly influential role for the nonphosphorylating glyceraldehyde-3-phosphate dehydrogenase, a cytosolic enzyme whose role in plants remains unclear. Our observations add new information on relationships between high CO_2 and oxidative signaling and provide novel insight into plant stress responses in conditions of increased CO_2.

Plants elaborate their cellular matter by generating carbon skeletons from atmospheric CO_2, the substrate for photosynthesis. Tropospheric CO_2 concentrations have been increasing for the last two centuries as a result of human activities. They are currently about 400 μL L^{-1} and are predicted to continue to increase over the coming years (Long and Ort, 2010). Many studies have sought to assess the impact of increased CO_2 levels on photosynthetic performance and plant yield within the wider objectives of predicting agricultural productivity and identifying appropriate varieties for growth in future conditions (Leakey et al., 2009; Long and Ort, 2010; Bishop et al., 2015). One key uncertainty concerns how increased CO_2, and the accompanying climatic changes, will affect plant responses to stress.

Although the question has received attention for many years (Manning and von Tiedemann, 1995), information on the potential impact of increased CO_2 on plant susceptibility to pathogen attack remains fragmentary. Both positive and negative effects of increased CO_2 on plant susceptibility to disease have been reported (McElrone et al., 2005; Lake and Wade, 2009; Melloy et al., 2010; Eastburn et al., 2011; Pangga et al., 2011). Several factors may account for the apparent conflict. Specific plant-pathogen interactions may be affected differently by high CO_2, and any one interaction may be influenced by CO_2 levels in multiple ways. Increased CO_2 could influence plant disease resistance by altering the nutritional value of plant tissues, by modifying pathways involved in plant resistance, or by modulating pathogen vigor and virulence (Hibberd et al., 1996; Lake and Wade, 2009; Melloy et al., 2010, 2014; Helfer, 2014; Zhang et al., 2015). During long-term exposure to increases in CO_2 in an agronomic setting, secondary effects could result from changes in plant development or canopy density (Eastburn et al., 2010, 2011). Modified stomatal opening or density is another factor by which altered CO_2 levels could affect the ability of pathogens to colonize plants (McElrone et al., 2005; Li et al., 2015).

The activation of inducible pathways allows plants to resist pathogenic invaders. Key players are the production of secondary compounds such as salicylic acid (SA) and phytoalexins (Glawischnig, 2007; Vlot et al., 2009). Primary metabolic status also can be an important factor in determining resistance to pathogens (Liu et al., 2010; Siemens et al., 2011; Stuttmann et al.,

[1] This work was supported by CYNTHIOL ANR (grant no. ANR12–BSV6–0011).

[2] Present address: Department of Plant Systems Biology, VIB, and Department of Plant Biotechnology and Bioinformatics, Ghent University, 9052 Ghent, Belgium.

* Address correspondence to graham.noctor@u-psud.fr.

The author responsible for distribution of materials integral to the findings presented in this article in accordance with the policy described in the Instructions for Authors (www.plantphysiol.org) is: Graham Noctor (graham.noctor@u-psud.fr).

A.M. and G.N. conceived the project and designed the experiments together; A.M. performed the experiments, processed the data, and produced the figures; A.M. and G.N. interpreted the data and wrote the article together.

[OPEN] Articles can be viewed without a subscription.

www.plantphysiol.org/cgi/doi/10.1104/pp.16.01129

2011). Primary plant carbon and nitrogen compounds are sought by invading pathogens as nutrients; they also are the biosynthetic precursors of the plant secondary metabolites that are required for resistance. Therefore, the effects of high CO_2 on primary metabolic pathways could feed forward to modify the production of defense compounds.

Evidence that the effects of increased CO_2 extend well beyond primary metabolism comes from transcriptomics studies performed in Arabidopsis (*Arabidopsis thaliana*), poplar (*Populus* spp.), soybean (*Glycine max*), and wheat (*Triticum aestivum*). Inspection of available data sets shows that high CO_2 impacts genes involved in secondary metabolism, hormone-dependent processes, redox regulation, and pathogenesis-related (PR) responses (Ainsworth et al., 2006; Li et al., 2008; Leakey et al., 2009; Tallis et al., 2010; Kane et al., 2013; Niu et al., 2016). Despite this, there have been very few detailed studies focused on how high CO_2 modulates plant defense pathways. Growth at high CO_2 increases SA in tomato (*Solanum lycopersicum*) and soybean (Casteel et al., 2012; Huang et al., 2012; Zhang et al., 2015). Certain secondary metabolites also were increased in tobacco (*Nicotiana tabacum*) grown at high CO_2, although only very slight effects on SA were observed (Matros et al., 2006). The pathways that might link enhanced CO_2 and the modified accumulation of defense compounds remain to be elucidated.

Our aim in this study was to explore the potential impact of high CO_2 on pathways involved in biotic stress resistance and related processes in plants. Because of the knowledge and genetic tools available in Arabidopsis, we focused the study on this species growing under controlled conditions. We report that the growth of plants in a CO_2-enriched environment is sufficient to prime multiple defense pathways and to increase resistance to pathogen challenge. Analysis of gene-specific mutants allowed us to define the underlying mechanisms more closely. The data identify a role for redox signaling processes in linking high-CO_2-triggered changes in metabolism to the activation of pathogen resistance pathways.

RESULTS

Because SA is an important compound in plant responses to pathogens, we quantified the effect of 1,000 μL L^{-1} CO_2 on this compound in Arabidopsis and three selected crop species growing in the absence of biotic challenge. When the Arabidopsis ecotype Columbia-0 (Col-0) was grown at this concentration of CO_2, significant accumulation of SA was observed in the leaves compared with plants grown in air (Fig. 1). High CO_2 caused a similar relative increase in SA contents in the Arabidopsis ecotype Wassilewskija, although absolute levels were lower than in Col-0 at both CO_2 regimes (Fig. 1). Under the same growth conditions, high CO_2 also increased SA in two varieties of bean (*Phaseolus vulgaris*) and, to some extent, in wheat. No significant effect was observed in barley (*Hordeum vulgare*; Fig. 1). To enable the use of gene-specific mutants to elucidate the processes underlying the increases in SA, we focused the rest of the study on the Arabidopsis Col-0 background.

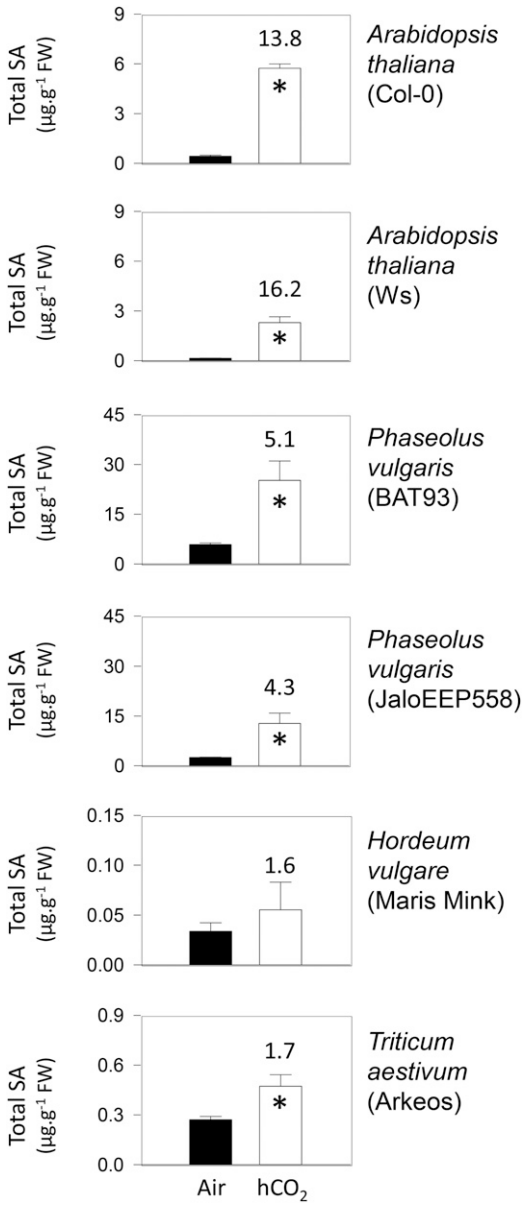

Figure 1. Effects of high CO_2 on the accumulation of SA in two Arabidopsis ecotypes (Col-0 and Wassilewskija [Ws]) and three different crop species. Plants were grown in 16-h days at an irradiance of 200 μmol m^{-2} s^{-1} for 3 weeks either in air (400 μL L^{-1}; black bars) or at high CO_2 (hCO_2; 1,000 μL L^{-1}; white bars). Data are means ± SE of four biological replicates. Numbers above the white bars indicate fold change for high CO_2-air. Significant differences between the conditions at $P < 0.05$ are indicated by asterisks. FW, Fresh weight.

Detailed Analysis of High-CO_2-Driven Activation of the SA Pathway and Its Consequences for Pathogen Resistance in Arabidopsis

To examine how rapidly mature plants grown in air or high CO_2 adjust to the other condition, a kinetic

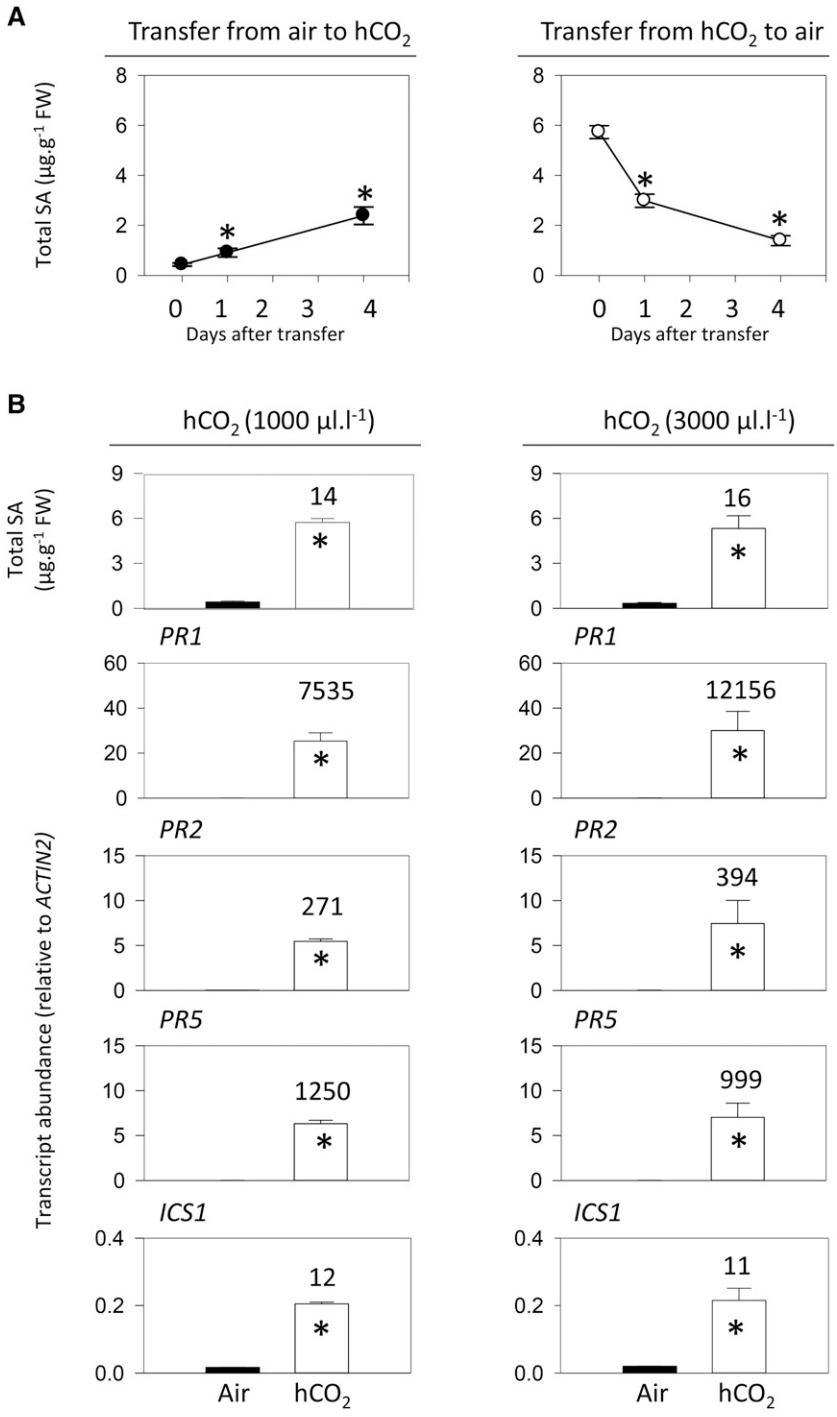

Figure 2. Kinetics of CO_2-dependent accumulation and removal of SA (A) and analysis of SA and SA-related gene expression in Arabidopsis Col-0 (B) at two different concentrations of high CO_2 (hCO_2). In A, plants were grown in 16-h days at an irradiance of 200 μmol m^{-2} s^{-1} for 18 d, either in air (left) or at high CO_2 (1,000 μL L^{-1}; right). At time 0, plants were transferred to the other condition, either high CO_2 (left) or air (right). Mean leaf SA contents in plants after 21 d continuous growth in air and high CO_2 were 0.32 ± 0.06 μg g^{-1} fresh weight (FW; n = three independent experiments, 10 biological replicates) and 5.86 ± 0.14 μg g^{-1} fresh weight (n = seven independent experiments, 24 biological replicates), respectively. In B, plants were grown from seed for 3 weeks either in air (black bars) or high CO_2 (white bars). At left, high CO_2 was 1,000 μL L^{-1}; at right, high CO_2 was 3,000 μL L^{-1}. Data are means ± SE of four (SA contents) or three (transcripts) biological replicates. Numbers above the bars indicate fold change for high CO_2-air. Significant differences between the conditions at $P < 0.05$ are indicated by asterisks.

analysis of changes in SA contents was performed. Plants were grown to the age of 18 d in air or 1,000 μL L^{-1} CO_2 and then shifted to the other condition for up to 4 d. Whereas shifting plants grown in air to high CO_2 caused SA to increase, SA decreased substantially in the days following the reverse shift. However, these CO_2-dependent changes in SA contents were relatively slow. In plants grown first in air and then transferred to high CO_2, significant SA accumulation was detectable within 1 d (Fig. 2A, left). Four days after transfer, SA had reached about half the level observed in plants grown in high CO_2 from seed (5.9 μg g^{-1} fresh weight; see Fig. 2 legend). When plants were grown from seed in high CO_2 and then transferred to air, SA was removed relatively quickly, returning almost to basal levels within 4 d (Fig. 2A, right).

To further characterize the effects of high CO_2 on SA-linked processes, we measured the key SA synthesis

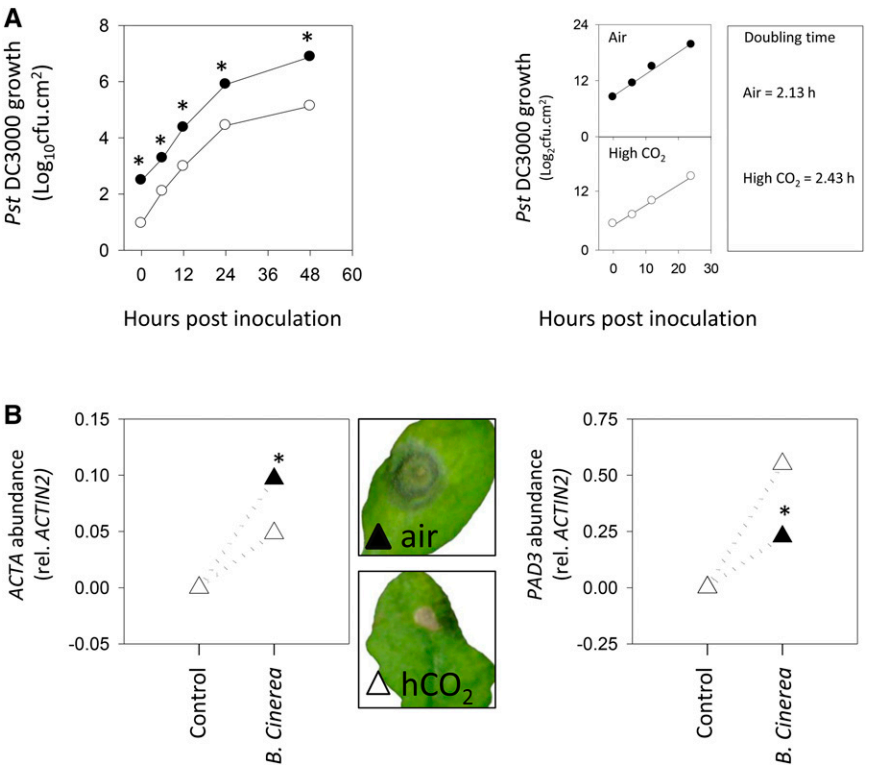

Figure 3. Effects of high CO_2 on Arabidopsis resistance to *Pto* and *Botrytis cinerea*. Col-0 was grown from seed in 16-h days at an irradiance of 200 μmol m^{-2} s^{-1} for 3 weeks either in air (400 μL L^{-1}; black symbols) or at high CO_2 (3,000 μL L^{-1}; white symbols) and then infected with *Pto* DC3000 or *B. cinerea* B05.10. A, Growth of *Pto* DC3000 in Col-0 leaves (left) and bacterial doubling time (right). cfu, Colony-forming units. B, Quantification of *B. cinerea ACTIN A* transcripts and photographs of infected leaves (left) and Arabidopsis *PAD3* transcripts in control and treated plants in air (black triangles) and high CO_2 (hCO_2; white triangles). Data are means ± SE of four (bacterial growth) or three (transcripts) biological replicates. Significant differences between the conditions at $P < 0.05$ are indicated by asterisks.

gene *ISOCHORISMATE SYNTHASE1* (*ICS1*) and three SA-dependent PR transcripts (Fig. 2B). This analysis was performed at 1,000 and 3,000 μL L^{-1} CO_2, in order to identify the concentrations required to saturate the responses. Both CO_2 regimes activated SA accumulation to a similar extent and induced *ICS1* expression to a similar level (Fig. 2B). At both 1,000 and 3,000 μL L^{-1} CO_2, *PR* genes were strongly induced (Fig. 2B). These results suggest that high CO_2 activates the accumulation of SA and SA-dependent transcripts and that a concentration of 1,000 μL L^{-1} is sufficient for this to occur. A concentration of 3,000 μL L^{-1} CO_2 had little further effect on SA and related factors. However, unless indicated otherwise, we performed the remainder of the study at this concentration, in order to make sure that the CO_2 effects on the SA pathway were saturating.

When Col-0 was challenged with the virulent pathogen *Pseudomonas syringae* pv *tomato* (*Pto*) DC3000, bacterial growth was significantly lower in plants that had been grown at high CO_2. A difference was already observed at time 0 (samples taken just after inoculation), suggesting that restricted bacterial entry into the leaves may underlie part of the apparent resistance (Fig. 3A). To attempt to account for this, the bacterial doubling time in planta was calculated over the first 24 h, revealing a higher value in plants grown in high CO_2 (Fig. 3A, right). As a second approach to circumvent problems associated with stomatal effects, we investigated the growth of the necrotrophic fungus *B. cinerea*. Unlike *Pto*, which in unwounded leaves gains access to the interior chiefly through stomata (Melotto et al., 2008), *B. cinerea* can enter by penetrating the cuticle. Lesion development and pathogen growth, as estimated by quantifying fungal *ACTIN A* transcripts, were lower in plants growing in high CO_2 than in air (Fig. 3B). This effect was associated with increased levels of transcripts for *PAD3*, an Arabidopsis gene implicated in resistance to *B. cinerea* (Ferrari et al., 2007). The activation of the SA pathway at high CO_2, therefore, is associated with enhanced resistance to both bacterial and fungal pathogens. Quantification of transcripts involved in jasmonic acid (JA) synthesis and signaling showed that the effect of high CO_2 is not restricted to the SA pathway (Supplemental Fig. S1).

Relationships of High-CO_2-Triggered PR Responses to Stomatal Regulation, Senescence, Metabolism, and Redox Signaling

Prolonged growth at high CO_2 can alter stomatal density (Eastburn et al., 2011), and it is well established that high CO_2 triggers stomatal closure in plants, including Arabidopsis (Long and Ort, 2010; Engineer et al., 2016). We examined the influence of stomatal regulation through a genetic approach. The *ost1* and *slac1* mutants have impaired stomatal regulation (Mustilli et al., 2002; Vahisalu et al., 2008). OPEN STOMATA1 (OST1) is a protein kinase that phosphorylates SLOW ANION CHANNEL1 (SLAC1) to activate stomatal closure. Loss of function of either component disables stomatal closure in response to a range of stimuli, including high CO_2 (Merilo et al., 2013). When *ost1* and *slac1* were grown at 1,000 and 3,000 μL L^{-1} CO_2,

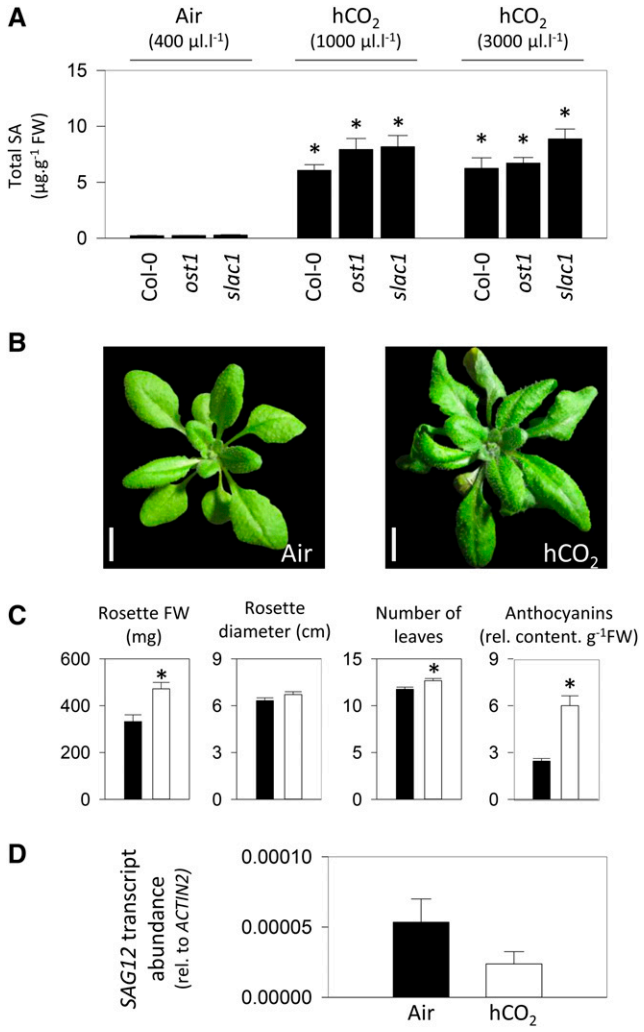

Figure 4. Investigation of the potential influence of stomatal function and leaf senescence in high-CO_2 (hCO_2)-induced pathogenesis responses. A, SA contents in Col-0 and two mutants impaired in stomatal closure (*ost1* and *slac1*) grown as in Figure 2B. B to D, Photographs, growth parameters, and *SAG12* transcript abundance in Col-0 grown in air and at high CO_2 as in Figure 3. In C and D, black and white bars represent growth at air and high CO_2, respectively. Data are means ± SE of 12 (growth parameters), four (SA), or three (*SAG12* transcripts) biological replicates. Significant differences between the conditions at $P < 0.05$ are indicated by asterisks. FW, Fresh weight. Bars in B = 1 cm.

they accumulated SA to levels similar to those in Col-0 (Fig. 4A).

Despite the accumulation of SA, no lesions were apparent on the leaves of Col-0 grown at high CO_2 (Fig. 4B). An increase in rosette mass was associated with increased anthocyanin content and a curling leaf phenotype (Fig. 4, B and C). Activation of senescence-related processes was assessed by the quantification of *SAG12* transcripts. In plants grown in either air or high CO_2, expression of this senescence marker remained at very low levels (Fig. 4D).

Gas chromatography-mass spectrometry analysis was used to assess the effects of high CO_2 on leaf metabolism by profiling about 80 compounds involved in carbon and nitrogen metabolism (Fig. 5; Supplemental Table S1). Metabolite profiles in the two conditions were clearly different, mainly caused by statistically significant increases in more than 20 compounds at high CO_2 compared with air. Among these compounds were several sugars, notably Fru, organic acids such as gluconic acid and citrate, and amino acids like Glu, Gln, Arg, and Phe (Fig. 5). The only metabolite that was decreased significantly at high CO_2 was Gly (Fig. 5A). A comparison with metabolite profiles obtained from multiple analyses of an oxidative stress background (*cat2*; Noctor et al., 2015) pointed toward some overlap between the effects of high CO_2 and intracellular redox perturbation (Fig. 5C), leading us to investigate this point further.

Reactive oxygen species (ROS) are notoriously difficult to quantify in an unambiguous manner (Noctor et al., 2015). Therefore, we explored the link between high CO_2 and redox factors in two alternative, more reliable ways (Noctor et al., 2016). First, we quantified antioxidants and pyridine nucleotides as markers of intracellular redox status. This analysis revealed that high CO_2 did not lead to marked perturbation of the redox states of these compounds. However, high CO_2 did increase total glutathione pools as well as NADPH contents (Fig. 6A). Second, we quantified transcripts for four oxidative signaling markers as well as the two major RboH-type NADPH oxidases expressed in leaves (Torres et al., 2006). All six of these transcripts were significantly more abundant in plants grown at high CO_2, pointing to the activation of oxidative signaling in these conditions (Fig. 6B).

Dissection of the High-CO_2-Triggered PR Responses Using Loss-of-Function Redox Mutants

Plants can produce SA from chorismate through two routes, one involving isochorismate, the other involving Phe (Garcion et al., 2008). The *sid2* mutant fails to accumulate SA in response to pathogens because it is deficient in ICS1 activity (Nawrath and Métraux, 1999; Wildermuth et al., 2001). We investigated whether high CO_2-induced *PR* responses also depend on this enzyme. As well as *ICS1* and *PR1* transcripts, we measured free and total SA as well as camalexin, an Arabidopsis phytoalexin (Glawischnig, 2007), in the wild type and *sid2*. The data show that high CO_2 triggers substantial increases in all these factors in Col-0 but not in *sid2*, in which values remained close to those observed in air (Fig. 7). As in Col-0, rosette mass was increased in *sid2* grown at high CO_2. Interestingly, the percentage increase was somewhat greater (Fig. 7). Whereas the mean rosette mass of Col-0 grown in high CO_2 was increased 42% relative to the value in air, the increase in *sid2* was 95%.

Because glutathione contents were increased at high CO_2 (Fig. 6) and this compound is implicated in responses to stress, including biotic challenge (Gomez et al., 2004; Parisy et al., 2007; Maughan et al., 2010; Han

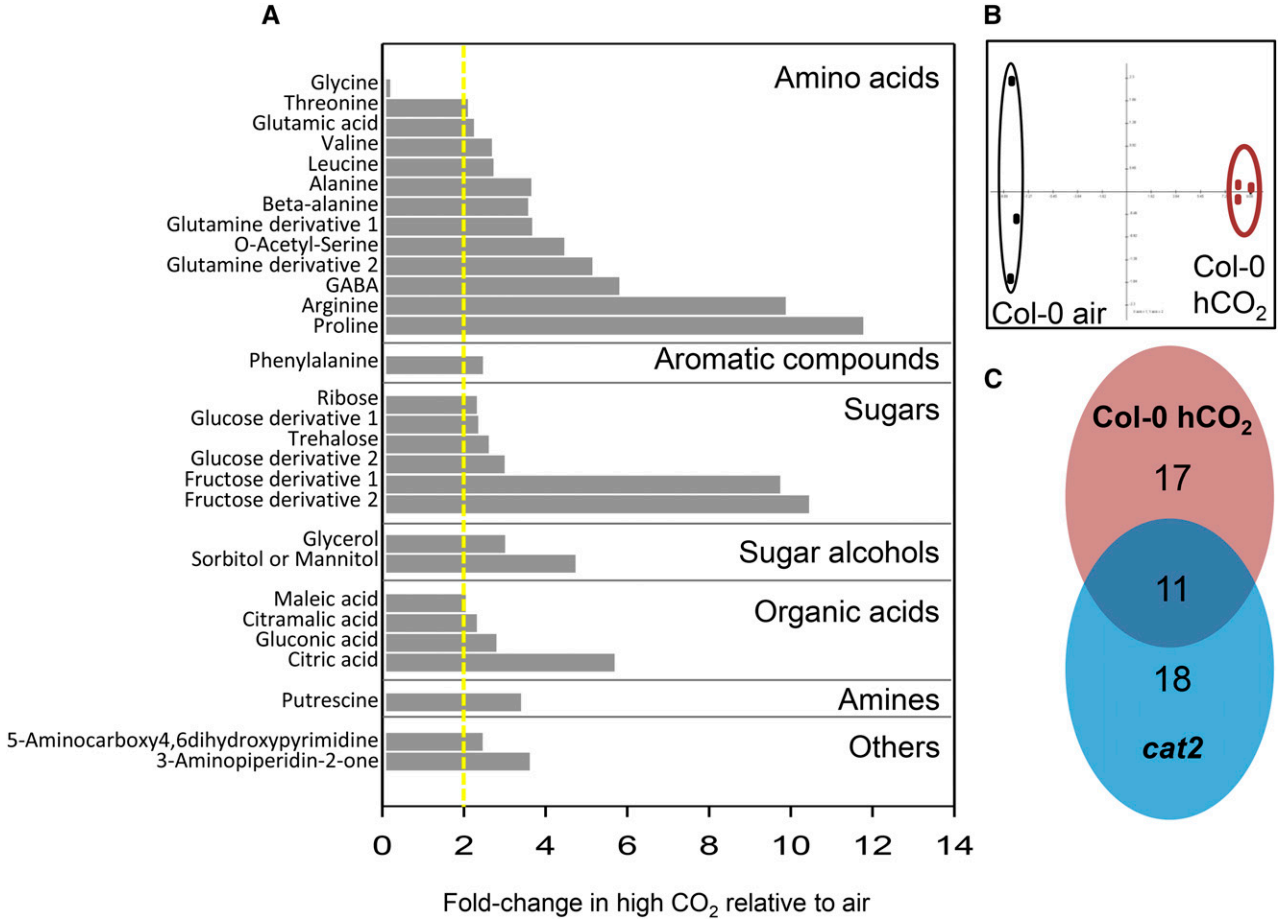

Figure 5. Impact of high CO_2 on gas chromatography-mass spectrometry metabolite profiles in Arabidopsis Col-0 leaves. A, Metabolites that showed significant differences between air and high CO_2 ($P < 0.05$; $n = 3$ biological replicates) and that were repressed or induced at least 2-fold (the dotted yellow line indicates a 2-fold increase in high CO_2). GABA, γ-Aminobutyrate. B, Principal component analysis of air and high-CO_2 (hCO_2) samples. C, Comparison of high-CO_2 effects (red) with oxidative stress effects (*cat2*; blue). Plants were grown as in Figure 3.

et al., 2013a, 2013b), we analyzed high-CO_2-triggered PR responses in two glutathione-deficient mutants. In agreement with previous analyses of plants grown in air (Parisy et al., 2007; Han et al., 2013a), glutathione contents were markedly lower in *pad2* and *cad2* than in Col-0 when plants were grown at high CO_2 (Fig. 8). Glutathione deficiency was not accompanied by substantial changes in ascorbate and pyridine nucleotides, other key biochemical markers of the redox state (Fig. 8A). Although glutathione deficiency did not affect leaf SA accumulation triggered by high CO_2, it did decrease expression of the SA signaling marker *PR1* in these conditions. *PR1* transcripts in *pad2* and *cad2* were intermediate between the levels in Col-0 and *sid2* (Fig. 8B). Compromised induction of *PR1* was accompanied by enhanced sensitivity to *Pto* DC3000, with bacterial growth also being intermediate between Col-0 and *sid2* (Fig. 8C).

NADPH generation in the cytosol is required for several processes related to PR responses, including glutathione reduction, NPR1 activation, and NADPH oxidase function. As noted above, sugars and some organic acids such as citrate were increased at high CO_2 (Fig. 5), and this was accompanied by increases in NADPH contents (Fig. 6). Therefore, we investigated the potential role of three cytosolic respiratory NADPH-generating enzymes in linking high CO_2 to activation of the SA pathway (Fig. 9A). Previously characterized mutants for isocitrate dehydrogenase (*icdh*), nonphosphorylating glyceraldehyde-3-phosphate dehydrogenase (*np-gapdh*), and NADP-MALIC ENZYME2 (*nadp-me2*) were exploited (Rius et al., 2006; Mhamdi et al., 2010; Voll et al., 2012; Li et al., 2013). We rechecked the levels of the relevant transcripts in the mutants and confirmed that all three are knockouts or severe knockdowns (Supplemental Fig. S2). This analysis also revealed some compensatory increases in expression of the genes encoding the other enzymes in *nadp-me2* and *np-gapdh*, although these adjustments were minor (Supplemental Fig. S2). None of the mutations had a marked effect on rosette mass when plants were grown in air, although *np-gapdh* was slightly smaller than the wild type

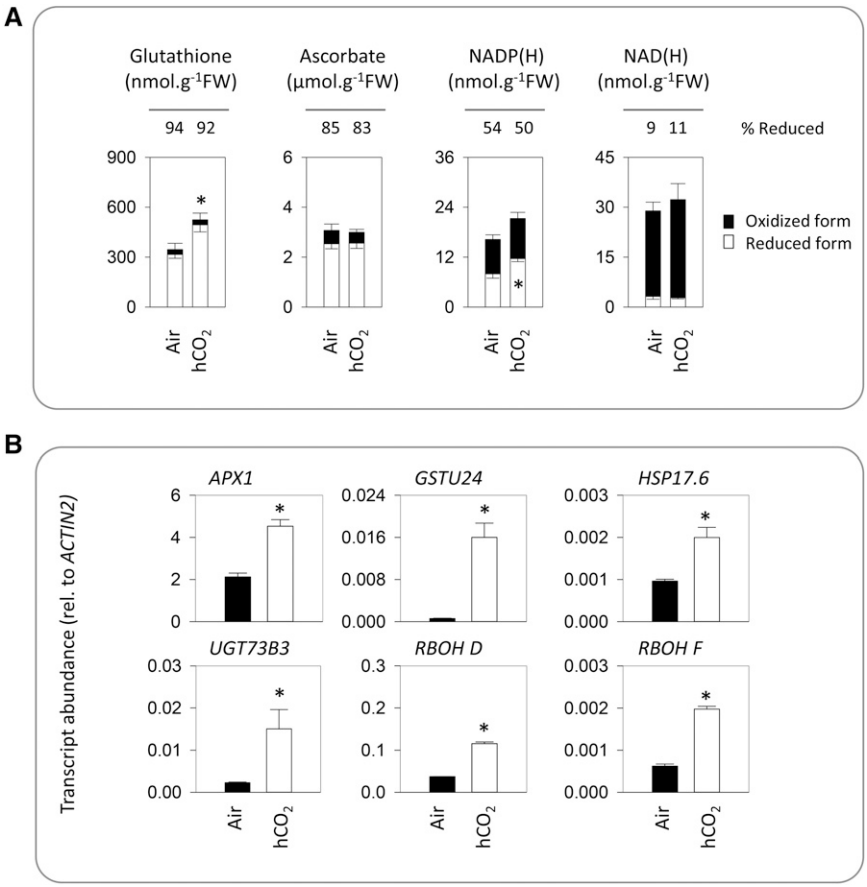

Figure 6. Redox profiles and ROS signaling in high CO_2 (hCO_2). Plants were grown as in Figure 3. A, Major antioxidants and pyridine nucleotides. White bars indicate reduced forms, and black bars indicate oxidized forms. Data are means ± SE of four biological replicates. Redox states are indicated above the bars as the percentage of each compound found in the reduced form. Significant differences between conditions at $P < 0.05$ were found in total glutathione content and NADPH (reduced form), as indicated by asterisks. No significant differences in reduction states were found. FW, Fresh weight. B, Abundance of transcripts for ROS-inducible genes and NADPH oxidases. Data are means ± SE of three biological replicates. Significant differences between the conditions at $P < 0.05$ are indicated by asterisks.

(Supplemental Fig. S3). This effect was more pronounced in plants grown at high CO_2, where *np-gapdh* produced only about 60% of the mass of the other three genotypes (Supplemental Fig. S3).

The impact of these mutations on defense metabolite profiles was analyzed. For this, we grew plants at high CO_2 and analyzed the contents of free and total forms of SA and scopoletin, a defense-related coumarin that is an important phytoalexin in tobacco (Chong et al., 2002), as well as camalexin. In these conditions, all three mutations negatively affected the accumulation of at least one of these compounds. The biggest impact was observed for the loss of *np-GAPDH* function, which caused all compounds to accumulate to significantly lower levels than in the wild type (Fig. 9B). To assess the impact of these effects on pathogen resistance, the growth of *Pto* DC3000 and *B. cinerea* was compared in the wild type and mutants grown at high CO_2. While the loss of *ICDH* function produced little effect on resistance to either pathogen, bacterial growth was increased significantly in *np-gapdh* and *nadp-me2* mutants (Fig. 10A). A similar effect was observed on fungal growth, with the *np-gapdh* mutant showing the biggest loss of resistance (Fig. 10B). Quantification of major redox pools in the same high-CO_2 conditions did not detect substantial effects of any of the mutations, although the *np-gapdh* mutant did show slight, significant increases in ascorbate and NAD(H) pools (Supplemental Fig. S4).

DISCUSSION

Despite the potentially profound effects of high CO_2 on diverse aspects of carbon metabolism, there have been few studies focused on how this condition modulates defense-related secondary compounds and related gene expression. The present report shows that growing Arabidopsis at 2.5 times current atmospheric CO_2 levels is sufficient to activate a wide range of PR responses and to prime resistance to biotic stress.

Comparison between High-CO_2- and Pathogen-Induced Defense Signaling

Significant increases in SA contents during growth at high CO_2 have been reported in tobacco, soybean, and tomato (Matros et al., 2006; Casteel et al., 2012; Huang et al., 2012; Zhang et al., 2015). Our results confirm these observations in other crop species and in Arabidopsis. How substantial is the accumulation of SA in Arabidopsis grown at high CO_2? According to our previous analyses of plants grown in air in otherwise identical conditions to those employed here, bacterial challenge (*Pto*) or sustained intracellular

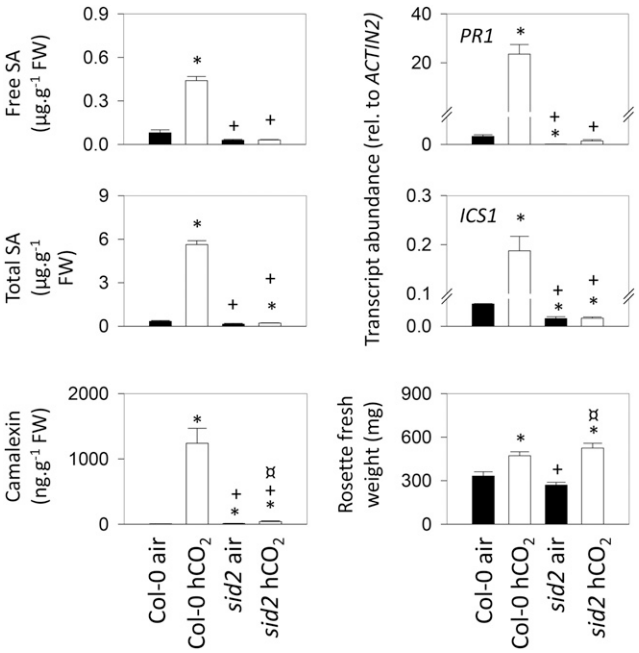

Figure 7. Comparison of high-CO_2 (hCO_2) responses in Col-0 and the *sid2* mutant. Plants were grown as in Figure 3. Asterisks indicate significant differences at $P < 0.05$ relative to Col-0 grown in air; plus signs indicate significant differences at $P < 0.05$ relative to Col-0 grown in high CO_2; and crossed circles indicate significant differences at $P < 0.05$ relative to *sid2* grown in air. FW, Fresh weight.

oxidative stress drives total leaf SA contents to at least 20 μg g^{-1} fresh weight (Chaouch et al., 2012). This compares with values of around 6 μg g^{-1} fresh weight triggered by high CO_2. Thus, it seems that the effect of high CO_2 is to prime PR responses rather than to activate them fully. Accumulation of SA in high CO_2 appears to be much slower than in response to pathogen challenge (Fig. 2), when this compound may accumulate markedly in less than 1 d (Chaouch et al., 2012). This slow response to CO_2 may be important to prevent the inappropriate activation of defenses in current atmospheric conditions, given that leaf intercellular CO_2 concentrations can vary widely throughout the day/night cycle as the relative importance of photosynthesis and respiration changes (Engineer et al., 2016).

Although the accumulation of SA triggered by high CO_2 was slower and less marked than that driven by biotic challenge, it appears to occur through the same pathways. High-CO_2-triggered increases in SA were associated with the induction of *ICS1* (Fig. 2). Most strikingly, the effects of high CO_2 on SA accumulation, SA-dependent gene expression, and resistance to *Pto* were annulled by the *sid2* mutation in this gene (Figs. 7 and 8). Thus, neither ICS2 nor the phenylalanine ammonia lyase (PAL) pathway appears to be required for increases in SA induced by elevated CO_2. However, several aspects of our data suggest that PAL-dependent pathways may be promoted by the increased carbon that is available in this condition. First, Phe itself was increased significantly, perhaps suggesting an activation of the shikimate pathway. Second, scopoletin, a coumarin that is derived from Phe, was markedly accumulated in Arabidopsis, in agreement with a previous study in tobacco (Matros et al., 2006). Third, we observed significantly increased anthocyanins. This last observation is consistent with high-CO_2 effects on the expression of anthocyanin synthesis genes in poplar (Tallis et al., 2010). Finally, we note that increases in extractable PAL activity and lignin contents have been reported in tobacco grown at 1,000 μL L^{-1} CO_2 (Matros et al., 2006).

While previous studies reporting high-CO_2-induced increases in SA have described unchanged or diminished contents of JA (Casteel et al., 2012; Huang et al., 2012; Zhang et al., 2015), we observed that both pathways were up-regulated together in Arabidopsis. The induction of these pathways by increased CO_2 is accompanied by enhanced resistance to both *Pto* and *B. cinerea*, the latter observation contrasting with results obtained in tomato, in which high CO_2 was reported to substantially increase sensitivity to the fungus (Zhang et al., 2015). Together with the increase in recognized phytoalexins, our data suggest that high CO_2 has the potential to activate a spectrum of plant defense responses that depend on secondary metabolism in Arabidopsis. While much attention has focused on the antagonism between JA and SA in terms of specific responses to different biotic stressors, conditions such as intracellular oxidative stress are able to activate both pathways simultaneously (Han et al., 2013a, 2013b). The ability of high CO_2 to induce both signaling pathways may suggest that oxidative stress is at the origin of the effect and that the unchanged redox states of biochemical markers like ascorbate and glutathione (Fig. 6A) reflect acclimation to this stress, possibly through the induction of antioxidative enzymes (Fig. 6B). The accumulation of SA may be part of the acclimation process to high CO_2, given that this compound can act to propagate oxidation or promote redox homeostasis, possibly in a concentration-dependent manner (Mateo et al., 2006; Vlot et al., 2009).

As noted above, high CO_2 activated defense pathways sufficiently to increase resistance to *Pto* and *B. cinerea*, and this occurred without lesion formation. In Arabidopsis Col-0, rosette mass was increased relative to growth in air, consistent with the stimulatory effects of high CO_2 in various C_3 species grown under controlled conditions (Long and Ort, 2010). In the *sid2* mutant, in which activation of the SA pathway was abolished, rosette mass was almost doubled by high CO_2, whereas a smaller fold increase was apparent in the wild type. Hence, the activation of defense pathways by high CO_2 in Arabidopsis (and possibly other plants) may be associated with some growth penalty. This perhaps suggests that high CO_2 may stimulate biomass production in the wild type less than it would if defense pathways were not activated.

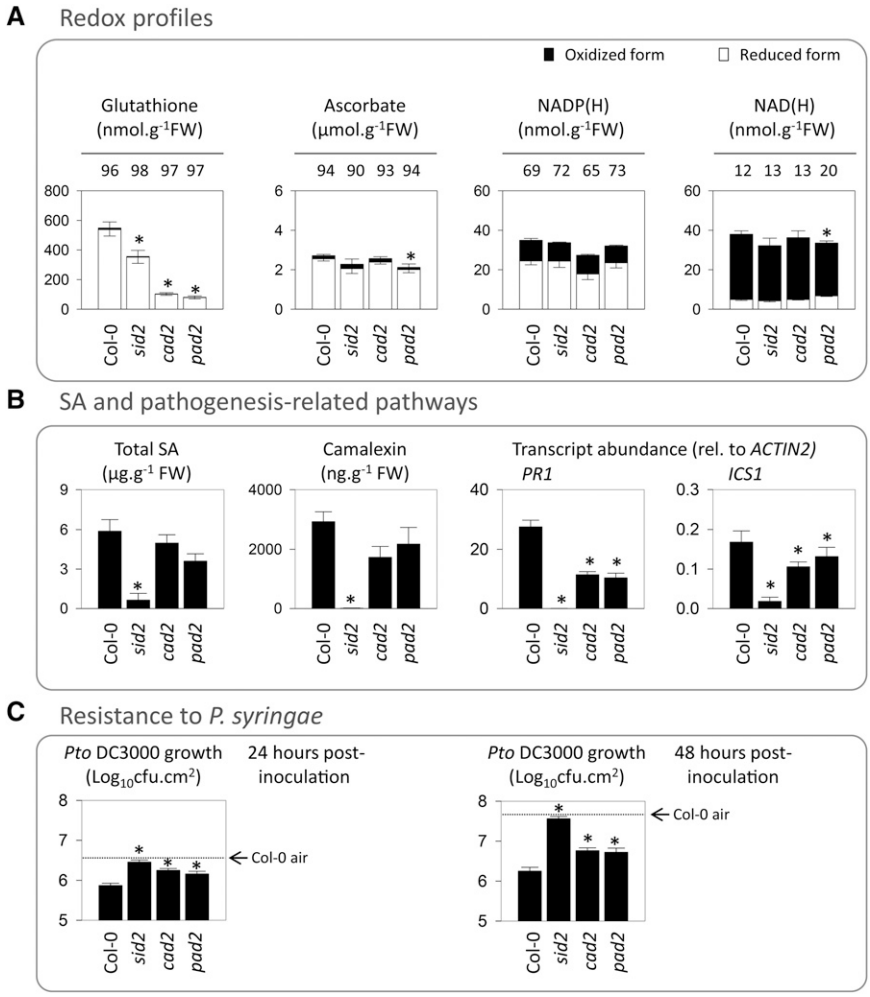

Figure 8. Analysis of the role of glutathione in high-CO_2-induced PR responses. A, Redox profiles in Col-0, *sid2*, *cad2*, and *pad2* grown at high CO_2. Redox states are indicated above the bars as the percentage of each compound found in the reduced form. Significant differences in total pools from Col-0 at $P < 0.05$ are indicated by asterisks. No significant differences in reduction states were found. FW, Fresh weight. B, SA, camalexin, and PR transcripts in the four genotypes grown at high CO_2. C, Growth of *Pto* DC3000 in Col-0 and different mutant lines at 24 and 48 h after inoculation grown at high CO_2. Plants were grown at high CO_2 as in Figure 3. Data are means ± SE of three (transcripts) or four (metabolites and bacterial growth) biological replicates. Asterisks indicate significant differences at $P < 0.05$ relative to Col-0. cfu, Colony-forming units.

High CO_2 Induces Biotic Stress Responses Independently of Stomatal Regulation or Senescence

Numerous factors regulate stomatal opening. As well as environmental conditions that are monitored by the plant to allow appropriate management of CO_2 entry and water loss, stomatal regulation is intertwined with responses to certain pathogens. Some bacteria can hijack plant signaling pathways to force stomatal opening, thereby aiding their entry into the plant (Melotto et al., 2006, 2008). Therefore, we examined whether the induction of PR responses by high CO_2 might be explained by mechanisms triggered by stomatal closure. Indeed, it is striking that the induction of PR responses was not substantially greater at 3,000 than at 1,000 μL L^{-1}. This is similar to the response of stomata to enhanced CO_2 in Arabidopsis. Stomatal conductance in Col-0 decreases about 50% after transfer from 400 to 800 μL L^{-1} CO_2 but does not decrease further after transfer to 2,000 μL L^{-1} (Hashimoto et al., 2006; Tian et al., 2015). While this points to the coordination of stomatal regulation and PR pathways by elevated CO_2, our analysis of *ost1* and *slac1* mutants provides no evidence of a direct mechanistic link between the two responses. Stomatal regulation in these mutants is insensitive to CO_2 up to at least 800 μL L^{-1} in *slac1* (Merilo et al., 2013) and up to 2,000 μL L^{-1} in *ost1* (Tian et al., 2015). Despite this, neither mutant showed any impairment of PR responses triggered by 1,000 or 3,000 μL L^{-1} (Fig. 4).

Age-related resistance, whereby plants become less susceptible to pathogens as they mature, has been described in Arabidopsis (Kus et al., 2002; Wilson et al., 2013). However, most evidence suggests that high CO_2 does not accelerate senescence. For instance, senescence-associated genes were repressed by high CO_2 in poplar, in contrast to the effect of oxidative stress triggered by ozone exposure (Kontunen-Soppela et al., 2010). In our study, the activation of defense pathways was not accompanied by increases in *SAG12* transcripts. Together with the absence of an obvious senescent phenotype at high CO_2, this suggests that the activation of PR responses is not linked to accelerated senescence.

While the stimulation of photosynthesis and plant growth by high CO_2 increases demand for other nutrients, our metabolite-profiling data provide no evidence that the observed activation of PR responses is linked to nitrogen limitation. Several key amino acids involved in primary nitrogen assimilation and storage (Glu, Gln,

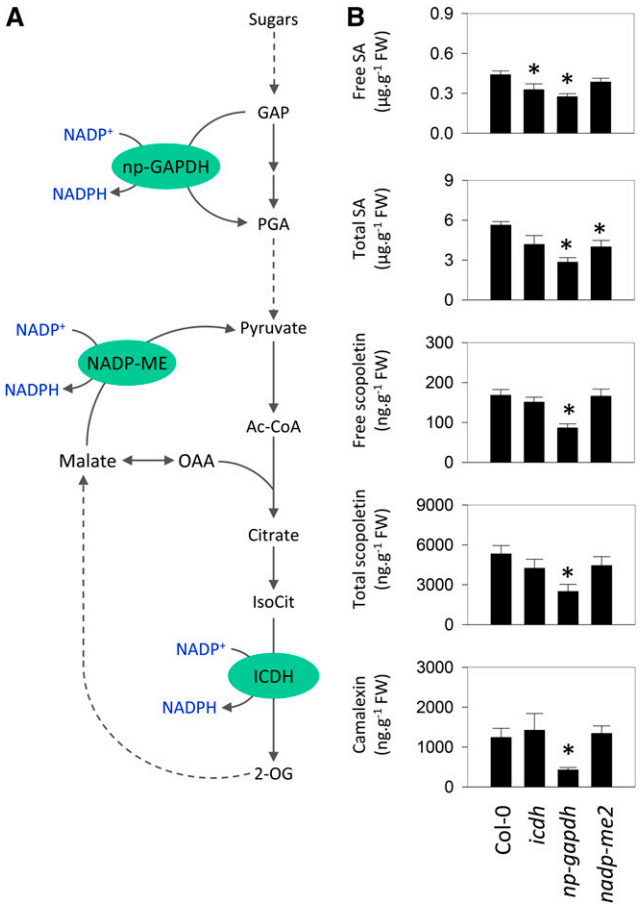

Figure 9. Roles of cytosolic NADP-dependent dehydrogenases in high-CO_2-triggered accumulation of SA and related defense compounds. A, Simplified scheme of glycolysis and the tricarboxylic acid cycle showing the reactions catalyzed by NADP-ICDH, NADP-ME2, and np-GAPDH. B, Defense compounds in Col-0 and knockout mutants grown at high CO_2 as in Figure 3. Data are means ± SE of nine biological replicates. Asterisks indicate significant differences from Col-0 at $P < 0.05$. AcCoA, Acetyl-CoA; FW, fresh weight; GAP, glyceraldehyde 3-phosphate; IsoCit, isocitrate; OAA, oxoloacetate; 2-OG, 2-oxoglutarate; PGA, 3-phosphoglycerate.

Ala, and Arg) were increased significantly at high CO_2. Gly was the only amino acid that was less abundant, consistent with decreased photorespiration at high CO_2 (Novitskaya et al., 2002). Interestingly, like alterations in sugar metabolism, changes in amino acid status can impact SA accumulation and pathogen susceptibility (Liu et al., 2010; Siemens et al., 2011; Stuttmann et al., 2011).

High CO_2 Triggers Oxidative Signaling

The relationship between high CO_2 and oxidative stress signaling remains unclear. One notion is that high CO_2 should mitigate oxidative stress because it inhibits photorespiration (which produces hydrogen peroxide in the peroxisomes) and also increases the supply of electron acceptors in the chloroplast. The latter effect is predicted to limit the leakage of electrons to oxygen by ensuring that $NADP^+$ regeneration is optimal (Foyer et al., 2012). If this is the case, oxidative signaling pathways should be down-regulated at high CO_2. By stark contrast, our data on ROS-related transcripts show that high CO_2 appears to activate oxidative signaling. This is in agreement with some data from transcriptomics analyses (Leakey et al., 2009; Niu et al., 2016). The induction of key enzymes such as APX may indicate an acclimatory response to potential oxidative stress at elevated CO_2, even if further work is required to identify the source of the stress and the pathways that link high CO_2 to activation of biotic defense pathways.

Although they accumulated SA, Arabidopsis plants grown at high CO_2 showed no lesions or decreased growth. Glutathione and ascorbate were at least as abundant at high CO_2 as in air, and in both conditions, these pools remained highly reduced. These observations do not point to marked oxidative stress in Arabidopsis grown at high CO_2. However, it is possible that the induction of oxidative signaling is linked to increases in ROS such as hydrogen peroxide and associated protein oxidation, which have been reported at high CO_2 (Cheeseman, 2006; Qiu et al., 2008). Another possible

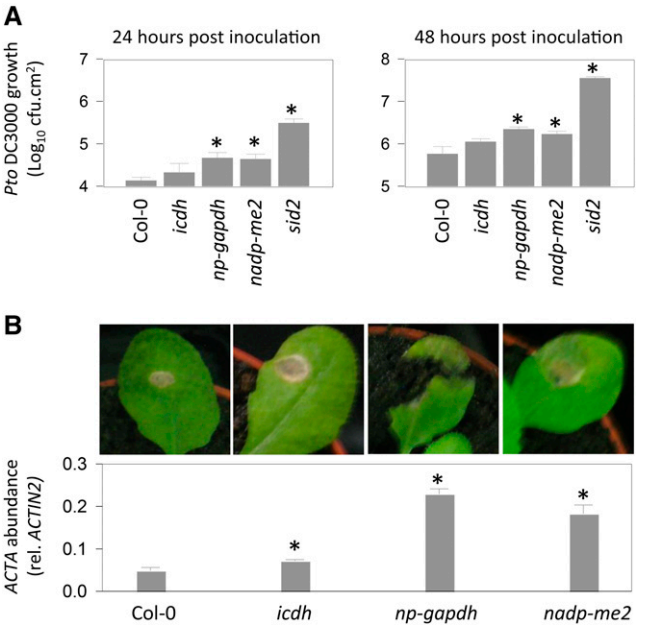

Figure 10. Resistance to pathogens in mutants for NADP-linked dehydrogenases. All experiments were performed on plants grown at high CO_2 as in Figure 3. A, Growth of *Pto* DC3000 in Col-0 and the mutant lines at 24 and 48 h after inoculation at high CO_2. The *sid2* mutant was included in the experiment for comparison. cfu, Colony-forming units. B, Representative photographs (top) and fungal *ACTIN A* transcript abundance (bottom) in leaves of Col-0 and mutants inoculated with *B. cinerea*. Data are means ± SE of three (B) or four (A) biological replicates. Asterisks indicate significant differences between infiltrated and control at $P < 0.05$.

factor may be a more oxidized cytosolic redox state in plants grown at high CO_2 because of diminished photorespiration (Bloom, 2015). However, as discussed further below, our data provide little evidence in favor of this explanation.

Glutathione Status and NADPH-Generating Enzymes Influence Pathogen Resistance Induced by High CO_2 through Different Mechanisms

Leaf glutathione contents modulate the accumulation of SA in response to oxidative stress (Han et al., 2013a). Interestingly, glutathione contents were enhanced significantly at high CO_2 (Fig. 6), and the accumulation of the Cys synthesis precursor, *O*-acetylserine (Fig. 5), suggests that this may have occurred through enhanced neosynthesis. However, based on SA and camalexin contents in glutathione-deficient mutants (Fig. 8), the induction of defense metabolites by high CO_2 does not seem to be regulated by glutathione concentration. Despite this, the induction of *PR* genes at high CO_2 was impaired by glutathione deficiency, as was resistance to *Pto*. According to current concepts, a likely explanation is that optimal glutathione levels are required to fully activate NPR1 downstream of SA accumulation (Vanacker et al., 2000; Gomez et al., 2004; Maughan et al., 2010).

Elevated CO_2 tends to stimulate respiration, particularly under nonlimiting nitrogen supply (Leakey et al., 2009; Markelz et al., 2014). In contrast to the lack of effect of glutathione deficiency on the accumulation of SA and camalexin at high CO_2, defense metabolite profiles were altered in mutants for cytosolic NADP-linked dehydrogenases. Relatively minor effects on free or total SA were observed for *icdh* and *nadp-me2* mutants, both of which have been implicated in defense responses and resistance to pathogens (Mhamdi et al., 2010; Voll et al., 2012). Our study reveals a role for this isoform of the malic enzyme in high-CO_2-triggered resistance to both bacteria and fungi (Fig. 10). The most novel aspect of the analysis is the sensitivity of the *np-gapdh* mutant, which showed decreased accumulation of all defense metabolites associated with compromised resistance to pathogen challenge in high CO_2 (Figs. 9 and 10). The existence of this enzyme in plants has been known for several decades (Kelly and Gibbs, 1973), yet its metabolic and biological functions remain unclear. A previous analysis of the mutant used here reported decreased growth (Rius et al., 2006). Our results confirm this effect and show that it is more marked at high CO_2 (Supplemental Fig. S3). Based on a consideration of likely in vivo substrate concentrations, and the properties of the NAD- and NADP-dependent GAPDHs, it has been proposed that np-GAPDH may contribute substantially to triose phosphate oxidation in the cytosol (Krömer, 1995). Cytosolic triose phosphate oxidation may be solicited increasingly at high CO_2, a condition that promotes photosynthetic carbon assimilation and that may favor faster triose phosphate export from the chloroplast through the phosphate translocator, which has been implicated in plastid-to-nucleus signaling in high-light conditions (Vogel et al., 2014). At high CO_2, the increased availability of triose phosphate should promote carbon and reductant delivery to the cytosol. Our data suggest that np-GAPDH may be a significant player during PR responses triggered in such conditions, where the production of increased respiratory substrates is favored (Fig. 9). This enzyme seems to be a part of metabolic/signaling networks that link high CO_2 to the production of secondary compounds involved in biotic stress resistance.

np-GAPDH and NADP-ME2 (the major cytosolic form in leaves) may be required to produce cytosolic reductant to fuel the activity of NADPH oxidases. However, none of the three mutants showed any significant difference in NADP(H) status from Col-0 (Supplemental Fig. S4). It is important to note that whole tissue measurements of NADP(H) may only give an approximate picture of the concentrations freely available to enzymes in vivo, because most of the pools that are detected in extracts may be bound at active sites at the moment of sampling (Hagedorn et al., 2004). Nevertheless, we cannot exclude that the dehydrogenase mutations impact high-CO_2-driven PR responses by altering metabolic factors other than NADP(H). For example, these enzymes could play roles in ensuring balance between different respiratory pathways, which may be important in the high-CO_2 response. Interestingly, respiratory metabolites such as citrate, whose signal was increased several-fold at high CO_2 (Fig. 5), have been reported to influence PR responses (Finkemeier et al., 2013).

CONCLUSION

High CO_2 is sufficient to prime plant defenses through processes that are linked partly to redox signaling and metabolism, and this can decrease sensitivity to infection. Our observations are relevant to several aspects of plant performance within agricultural contexts. They underscore the importance of nutritional factors in governing the outcome of plant-pathogen interactions (Kangasjärvi et al., 2012). Furthermore, the effect of high CO_2 on the expression of some genes involved in biotic stress responses can be conditioned by daylength or nutrient availability (Queval et al., 2012; Niu et al., 2016). In winter wheat that had not been cold hardened, high CO_2 repressed genes involved in biotic stress signaling, and this repression was less apparent in cold-hardened plants (Kane et al., 2013). All these studies underscore the complexity that could determine how the plant immune system responds to CO_2 in the natural or field environment.

Like most studies of the effects of high CO_2 on plants, this work does not simulate the naturally occurring increases in the atmospheric concentrations of this gas. These are slow and gradual, and plant responses will likely involve adaptation over many generations as

much as, if not more than, acclimation. Nevertheless, our data contribute to understanding the potential of plants to exploit the increased atmospheric CO_2 concentrations that are predicted through the coming decades. They also may have implications for ongoing attempts to engineer C_4 photosynthesis in plants that currently photosynthesize through the C_3 pathway. C_4 plants such as maize (*Zea mays*) have two well-defined photosynthetic cell types that maintain very different CO_2 concentrations, with the bundle sheath cells functioning in a high-CO_2 environment (Leegood, 2002). Antioxidative systems also are distributed differentially between the two cell types (Doulis et al., 1997). It could be interesting to explore the cellular specificity of pathogenesis responses in C_4 species and to compare them with responses in C_3 plants, in which photosynthetic cells do not have such a marked difference in CO_2 concentrations. Finally, our data also may be relevant to horticultural practices that involve the use of high CO_2 at the preharvest or postharvest stage of production. The cultivation of crops under glass often involves supplementation of CO_2 to increase photosynthesis (Jaffrin et al., 2003; Boulard et al., 2011), while high levels of CO_2 can be used during postharvest storage to restrict pathogen growth (Teles et al., 2014; Ruiz et al., 2016). Arabidopsis lends itself to genetic studies to further elucidate the links between enhanced CO_2 and biotic stress responses.

MATERIALS AND METHODS

Plant Material

Arabidopsis (*Arabidopsis thaliana*) ecotype Col-0 and T-DNA mutant lines were obtained from the European Arabidopsis Stock Centre (http://arabidopsis.info). All T-DNA lines have been reported in previous studies. The *icdh*, *np-gapdh*, and *nadp-me2* mutant lines were *icdh-1*, *np-gapdh*, and *nadp-me2-1*, as described, respectively, by Mhamdi et al. (2010), Rius et al. (2006), and Li et al. (2013). The *cad2* and *pad2* mutants are partly deficient in glutathione caused by mutations in the first committed enzyme of the glutathione synthesis pathway (Cobbett et al., 1998; Parisy et al., 2007). The *sid2* mutant was described originally by Nawrath and Métraux (1999) and is defective in ICS1 (Wildermuth et al., 2001). The stomatal regulation mutants were *slac1-4* (Vahisalu et al., 2008) and *ost1-1* (Mustilli et al., 2002). The common bean (*Phaseolus vulgaris*) genotypes were as in David et al. (2009) and were a gift from Valérie Geffroy (Institute of Plant Sciences Paris Saclay). Barley (*Hordeum vulgare*) and wheat (*Triticum aestivum*) seeds were gifts from Peter Lea (Lancaster University) and Emmanuelle Issakidis-Bourguet (Institute of Plant Sciences Paris Saclay), respectively.

Plant Growth and Sampling

Plants were grown in a controlled-environment growth room at a day/night regime of 16 h/8 h (light/dark), an irradiance of 200 μmol m^{-2} s^{-1} at leaf level, temperatures of 20°C day/18°C night, 65% humidity, and a CO_2 concentration of 400 μL L^{-1} (air), 1,000 μL L^{-1}, or 3,000 μL L^{-1}. Nutrient solution was supplied twice per week. Plants were harvested in the middle of the light period after 3 weeks of growth. Samples were quickly frozen in liquid nitrogen and stored at −80°C until analysis. All data were obtained from at least three biological replicates (for details, see figure legends). Technical repeats were performed for quantitative reverse transcription-PCR and the analysis of redox compounds. In all cases, mean values ± SE were obtained from a single data point obtained for each biological replicate, and significant differences between samples were evaluated using Student's *t* test at a confidence level of $P < 0.05$.

RNA Extraction and Gene Expression Analysis

Total RNA was extracted from plants grown in air or in high CO_2 using the Trizol reagent (Life Technologies). cDNA synthesis was performed using the SuperScript III First-Strand Synthesis System according to the manufacturer's instructions (Life Technologies). Quantitative reverse transcription-PCR analysis was performed as described by Mhamdi et al. (2010) using the gene-specific primer sequences listed in Supplemental Table S2.

Metabolite Quantification

Glutathione, ascorbate, and NAD(P)(H) were quantified using the plate-reader method described by Queval and Noctor (2007). Targeted analysis of SA, scopoletin, and camalexin was performed by HPLC-fluorescence as described by Chaouch et al. (2012). Nontargeted analysis of metabolites was performed by a gas chromatography-time of flight-mass spectrometry (GC-TOF-MS) method that allows the profiling of about 80 metabolites (Chaouch et al., 2012; Noctor et al., 2015). A detailed description of the GC-TOF-MS methodology was reported by Li et al. (2014), and a full list of metabolites is given in Supplemental Table S1.

Pathogen Tests

The resistance of plants to *Pseudomonas syringae* pv *tomato* strain DC3000 was examined as described by Chaouch et al. (2012) using a bacterial titer of 10^6 colony-forming units mL^{-1}. Bacteria were cultivated on medium with 100 mg L^{-1} rifampicin and 25 mg L^{-1} kanamycin and introduced into the middle leaves of plants using a 1-mL syringe without a needle. Samples were taken for analysis at 24 and 48 h postinoculation. Each sample consisted of two leaf discs, and quadruplicate biological samples were used in all cases. Discs were ground in water to extract bacteria, and colonies were counted after growth on agar plates for 3 d.

The effects of *Botrytis cinerea* on Arabidopsis plants were examined as described by Ferrari et al. (2003). Briefly, the *B. cinerea* strain B05.10 was activated for several cycles and grown on potato dextrose agar medium for 2 weeks. After sporulation, spores were suspended in one-half-strength liquid potato dextrose agar medium to 5×10^5 spores mL^{-1}. Resistance tests were performed by infection of three leaves from each plant with a 5-μL drop of the spore solution. Infected plants were incubated for 3 d under a transparent plastic cover to maintain high humidity.

Supplemental Data

The following supplemental materials are available.

Supplemental Figure S1. Quantitative PCR analysis of JA-associated genes in plants grown in air and high CO_2.

Supplemental Figure S2. Quantitative PCR analysis of major NADP dehydrogenase transcripts in Col-0 and the corresponding mutants grown at high CO_2.

Supplemental Figure S3. Phenotypes of Col-0 and NADP dehydrogenase mutants grown in air or at high CO_2.

Supplemental Figure S4. Effects of mutations in cytosolic NADP-linked dehydrogenase on intracellular redox markers.

Supplemental Table S1. Full list of metabolites and their relative contents analyzed by GC-TOF-MS.

Supplemental Table S2. Primer sequences used in this study.

ACKNOWLEDGMENTS

We thank the Salk Institute Genomic Analysis Laboratory for providing the sequence-indexed Arabidopsis T-DNA insertion mutants and the Nottingham Arabidopsis Stock Centre for supplying seed stocks; Jaakko Kangasjarvi (University of Helsinki) for providing *ost1* and *slac1* Arabidopsis seeds and Peter Lea (Lancaster University) for the barley seeds; and Valerie Geffroy, Audrey Chaix-Bryan, Emmanuel Issakidis-Bourget, Sophie Blanchet, and Patrick Saindrenan (Institute of Plant Sciences Paris Saclay) for the kind gifts of bean and wheat seeds and the B05.10 strain of *B. cinerea* as well as for advice on growth.

Received July 20, 2016; accepted August 29, 2016; published August 30, 2016.

LITERATURE CITED

Ainsworth EA, Rogers A, Vodkin LO, Walter A, Schurr U (2006) The effects of elevated CO_2 concentration on soybean gene expression: an analysis of growing and mature leaves. Plant Physiol **142:** 135–147

Bishop KA, Betzelberger AM, Long SP, Ainsworth EA (2015) Is there potential to adapt soybean (Glycine max Merr.) to future [CO_2]? An analysis of the yield response of 18 genotypes in free-air CO_2 enrichment. Plant Cell Environ **38:** 1765–1774

Bloom AJ (2015) The increasing importance of distinguishing among plant nitrogen sources. Curr Opin Plant Biol **25:** 10–16

Boulard T, Raeppel C, Brun R, Lecompte F, Hayer F, Carmassi G, Gaillard G (2011) Environmental impact of greenhouse tomato production in France. Agronomy for Sustainable Development **31:** 757–777

Casteel CL, Segal LM, Niziolek OK, Berenbaum MR, DeLucia EH (2012) Elevated carbon dioxide increases salicylic acid in *Glycine max*. Environ Entomol **41:** 1435–1442

Chaouch S, Queval G, Noctor G (2012) AtRbohF is a crucial modulator of defence-associated metabolism and a key actor in the interplay between intracellular oxidative stress and pathogenesis responses in Arabidopsis. Plant J **69:** 613–627

Cheeseman JM (2006) Hydrogen peroxide concentrations in leaves under natural conditions. J Exp Bot **57:** 2435–2444

Chong J, Baltz R, Schmitt C, Beffa R, Fritig B, Saindrenan P (2002) Downregulation of a pathogen-responsive tobacco UDP-Glc:phenylpropanoid glucosyltransferase reduces scopoletin glycoside accumulation, enhances oxidative stress, and weakens virus resistance. Plant Cell **14:** 1093–1107

Cobbett CS, May MJ, Howden R, Rolls B (1998) The glutathione-deficient, cadmium-sensitive mutant, *cad2-1*, of *Arabidopsis thaliana* is deficient in γ-glutamylcysteine synthetase. Plant J **16:** 73–78

David P, Chen NWG, Pedrosa-Harand A, Thareau V, Sévignac M, Cannon SB, Debouck D, Langin T, Geffroy V (2009) A nomadic subtelomeric disease resistance gene cluster in common bean. Plant Physiol **151:** 1048–1065

Doulis AG, Debian N, Kingston-Smith AH, Foyer CH (1997) Differential localization of antioxidants in maize leaves. Plant Physiol **114:** 1031–1037

Eastburn DM, Degennarow MM, DeLucia EH, Dermody O, McElrone AJ (2010) Elevated atmospheric carbon dioxide and ozone alter soybean diseases at SoyFACE. Glob Change Biol **16:** 320–330

Eastburn DM, McElrone AJ, Bilgin DD (2011) Influence of atmospheric and climatic change on plant-pathogen interactions. Plant Pathol **60:** 54–69

Engineer CB, Hashimoto-Sugimoto M, Negi J, Israelsson-Nordström M, Azoulay-Shemer T, Rappel WJ, Iba K, Schroeder JI (2016) CO_2 sensing and CO_2 regulation of stomatal conductance: advances and open questions. Trends Plant Sci **21:** 16–30

Ferrari S, Galletti R, Denoux C, De Lorenzo G, Ausubel FM, Dewdney J (2007) Resistance to *Botrytis cinerea* induced in Arabidopsis by elicitors is independent of salicylic acid, ethylene, or jasmonate signaling but requires *PHYTOALEXIN DEFICIENT3*. Plant Physiol **144:** 367–379

Ferrari S, Plotnikova JM, De Lorenzo G, Ausubel FM (2003) Arabidopsis local resistance to *Botrytis cinerea* involves salicylic acid and camalexin and requires EDS4 and PAD2, but not SID2, EDS5 or PAD4. Plant J **35:** 193–205

Finkemeier I, König AC, Heard W, Nunes-Nesi A, Pham PA, Leister D, Fernie AR, Sweetlove LJ (2013) Transcriptomic analysis of the role of carboxylic acids in metabolite signaling in Arabidopsis leaves. Plant Physiol **162:** 239–253

Foyer CH, Neukermans J, Queval G, Noctor G, Harbinson J (2012) Photosynthetic control of electron transport and the regulation of gene expression. J Exp Bot **63:** 1637–1661

Garcion C, Lohmann A, Lamodière E, Catinot J, Buchala A, Doermann P, Métraux JP (2008) Characterization and biological function of the ISOCHORISMATE SYNTHASE2 gene of Arabidopsis. Plant Physiol **147:** 1279–1287

Glawischnig E (2007) Camalexin. Phytochemistry **68:** 401–406

Gomez LD, Noctor G, Knight MR, Foyer CH (2004) Regulation of calcium signalling and gene expression by glutathione. J Exp Bot **55:** 1851–1859

Hagedorn PH, Flyvbjerg H, Møller IM (2004) Modelling NADH turnover in plant mitochondria. Physiol Plant **120:** 370–385

Han Y, Chaouch S, Mhamdi A, Queval G, Zechmann B, Noctor G (2013a) Functional analysis of Arabidopsis mutants points to novel roles for glutathione in coupling H_2O_2 to activation of salicylic acid accumulation and signaling. Antioxid Redox Signal **18:** 2106–2121

Han Y, Mhamdi A, Chaouch S, Noctor G (2013b) Regulation of basal and oxidative stress-triggered jasmonic acid-related gene expression by glutathione. Plant Cell Environ **36:** 1135–1146

Hashimoto M, Negi J, Young J, Israelsson M, Schroeder JI, Iba K (2006) *Arabidopsis* HT1 kinase controls stomatal movements in response to CO_2. Nat Cell Biol **8:** 391–397

Helfer S (2014) Rust fungi and global change. New Phytol **201:** 770–780

Hibberd JM, Whitbread R, Farrar JF (1996) Effect of elevated concentrations of CO_2 in infection of barley by *Erysiphe graminis*. Physiol Mol Plant Pathol **48:** 37–53

Huang L, Ren Q, Sun Y, Ye L, Cao H, Ge F (2012) Lower incidence and severity of tomato virus in elevated CO_2 is accompanied by modulated plant induced defence in tomato. Plant Biol (Stuttg) **14:** 905–913

Jaffrin A, Bentounes N, Joan AM, Makhlouf S (2003) Landfill biogas for heating greenhouses and providing carbon dioxide supplement for plant growth. Biosystems Eng **86:** 113–123

Kane K, Dahal KP, Badawi MA, Houde M, Hüner NPA, Sarhan F (2013) Long-term growth under elevated CO_2 suppresses biotic stress genes in non-acclimated, but not cold-acclimated winter wheat. Plant Cell Physiol **54:** 1751–1768

Kangasjärvi S, Neukermans J, Li S, Aro EM, Noctor G (2012) Photosynthesis, photorespiration, and light signalling in defence responses. J Exp Bot **63:** 1619–1636

Kelly GJ, Gibbs M (1973) Nonreversible D-glyceraldehyde 3-phosphate dehydrogenase of plant tissues. Plant Physiol **52:** 111–118

Kontunen-Soppela S, Riikonen J, Ruhanen H, Brosché M, Somervuo P, Peltonen P, Kangasjärvi J, Auvinen P, Paulin L, Keinänen M, et al (2010) Differential gene expression in senescing leaves of two silver birch genotypes in response to elevated CO_2 and tropospheric ozone. Plant Cell Environ **33:** 1016–1028

Krömer S (1995) Respiration during photosynthesis. Annu Rev Plant Physiol Plant Mol Biol **46:** 45–70

Kus JV, Zaton K, Sarkar R, Cameron RK (2002) Age-related resistance in *Arabidopsis* is a developmentally regulated defense response to *Pseudomonas syringae*. Plant Cell **14:** 479–490

Lake JA, Wade RN (2009) Plant-pathogen interactions and elevated CO_2: morphological changes in favour of pathogens. J Exp Bot **60:** 3123–3131

Leakey ADB, Xu F, Gillespie KM, McGrath JM, Ainsworth EA, Ort DR (2009) Genomic basis for stimulated respiration by plants growing under elevated carbon dioxide. Proc Natl Acad Sci USA **106:** 3597–3602

Leegood RC (2002) C_4 photosynthesis: principles of CO_2 concentration and prospects for its introduction into C_3 plants. J Exp Bot **53:** 581–590

Li P, Ainsworth EA, Leakey ADB, Ulanov A, Lozovaya V, Ort DR, Bohnert HJ (2008) Arabidopsis transcript and metabolite profiles: ecotype-specific responses to open-air elevated [CO_2]. Plant Cell Environ **31:** 1673–1687

Li S, Mhamdi A, Clement C, Jolivet Y, Noctor G (2013) Analysis of knockout mutants suggests that Arabidopsis *NADP-MALIC ENZYME2* does not play an essential role in responses to oxidative stress of intracellular or extracellular origin. J Exp Bot **64:** 3605–3614

Li S, Mhamdi A, Trotta A, Kangasjärvi S, Noctor G (2014) The protein phosphatase subunit PP2A-B′γ is required to suppress day length-dependent pathogenesis responses triggered by intracellular oxidative stress. New Phytol **202:** 145–160

Li X, Sun Z, Shao S, Zhang S, Ahammed GJ, Zhang G, Jiang Y, Zhou J, Xia X, Zhou Y, et al (2015) Tomato-Pseudomonas syringae interactions under elevated CO_2 concentration: the role of stomata. J Exp Bot **66:** 307–316

Liu G, Ji Y, Bhuiyan NH, Pilot G, Selvaraj G, Zou J, Wei Y (2010) Amino acid homeostasis modulates salicylic acid-associated redox status and defense responses in *Arabidopsis*. Plant Cell **22:** 3845–3863

Long SP, Ort DR (2010) More than taking the heat: crops and global change. Curr Opin Plant Biol **13:** 241–248

Manning WJ, von Tiedemann A (1995) Climate change: potential effects of increased atmospheric carbon dioxide (CO_2), ozone (O_3), and ultraviolet-B (UV-B) radiation on plant diseases. Environ Pollut **88:** 219–245

Markelz RJC, Lai LX, Vosseler LN, Leakey ADB (2014) Transcriptional reprogramming and stimulation of leaf respiration by elevated CO_2 concentration is diminished, but not eliminated, under limiting nitrogen supply. Plant Cell Environ **37:** 886–898

Mateo A, Funck D, Mühlenbock P, Kular B, Mullineaux PM, Karpinski S (2006) Controlled levels of salicylic acid are required for optimal photosynthesis and redox homeostasis. J Exp Bot **57:** 1795–1807

Matros A, Amme S, Kettig B, Buck-Sorlin GH, Sonnewald U, Mock HP (2006) Growth at elevated CO_2 concentrations leads to modified profiles of secondary metabolites in tobacco cv. SamsunNN and to increased resistance against infection with potato virus Y. Plant Cell Environ **29:** 126–137

Maughan SC, Pasternak M, Cairns N, Kiddle G, Brach T, Jarvis R, Haas F, Nieuwland J, Lim B, Müller C, et al (2010) Plant homologs of the Plasmodium falciparum chloroquine-resistance transporter, PfCRT, are required for glutathione homeostasis and stress responses. Proc Natl Acad Sci USA **107:** 2331–2336

McElrone AJ, Reid CD, Hoye KA, Hart E, Jackson RB (2005) Elevated CO_2 reduces disease incidence and severity of a red maple fungal pathogen via changes in host physiology and leaf chemistry. Glob Change Biol **11:** 1828–1836

Melloy P, Aitken E, Luck J, Chakraborty S, Obanor F (2014) The influence of increasing temperature and CO_2 on Fusarium crown rot susceptibility of wheat genotypes at key growth stages. Eur J Plant Pathol **140:** 19–37

Melloy P, Holloway G, Luck J, Norton R, Aitken E, Chakraborty S (2010) Production and fitness of *Fusarium pseudograminearum* inoculum at elevated carbon dioxide in FACE. Glob Change Biol **16:** 3363–3373

Melotto M, Underwood W, He SY (2008) Role of stomata in plant innate immunity and foliar bacterial diseases. Annu Rev Phytopathol **46:** 101–122

Melotto M, Underwood W, Koczan J, Nomura K, He SY (2006) Plant stomata function in innate immunity against bacterial invasion. Cell **126:** 969–980

Merilo E, Laanemets K, Hu H, Xue S, Jakobson L, Tulva I, Gonzalez-Guzman M, Rodriguez PL, Schroeder JI, Broschè M, et al (2013) PYR/RCAR receptors contribute to ozone-, reduced air humidity-, darkness-, and CO_2-induced stomatal regulation. Plant Physiol **162:** 1652–1668

Mhamdi A, Mauve C, Gouia H, Saindrenan P, Hodges M, Noctor G (2010) Cytosolic NADP-dependent isocitrate dehydrogenase contributes to redox homeostasis and the regulation of pathogen responses in *Arabidopsis* leaves. Plant Cell Environ **33:** 1112–1123

Mustilli AC, Merlot S, Vavasseur A, Fenzi F, Giraudat J (2002) *Arabidopsis* OST1 protein kinase mediates the regulation of stomatal aperture by abscisic acid and acts upstream of reactive oxygen species production. Plant Cell **14:** 3089–3099

Nawrath C, Métraux JP (1999) Salicylic acid induction-deficient mutants of *Arabidopsis* express PR-2 and PR-5 and accumulate high levels of camalexin after pathogen inoculation. Plant Cell **11:** 1393–1404

Niu Y, Ahammed GJ, Tang C, Guo L, Yu J (2016) Physiological and transcriptome responses to combinations of elevated CO_2 and magnesium in *Arabidopsis thaliana*. PLoS ONE **11:** e0149301

Noctor G, Lelarge-Trouverie C, Mhamdi A (2015) The metabolomics of oxidative stress. Phytochemistry **112:** 33–53

Noctor G, Mhamdi A, Foyer CH (2016) Oxidative stress and antioxidative systems: recipes for successful data collection and interpretation. Plant Cell Environ **39:** 1140–1160

Novitskaya L, Trevanion S, Driscoll SD, Foyer CH, Noctor G (2002) How does photorespiration modulate leaf amino acid contents? A dual approach through modelling and metabolite analysis. Plant Cell Environ **25:** 821–836

Pangga IB, Hanan J, Chakraborty S (2011) Pathogen dynamics in a crop canopy and their evolution under changing climate. Plant Pathol **60:** 70–81

Parisy V, Poinssot B, Owsianowski L, Buchala A, Glazebrook J, Mauch F (2007) Identification of PAD2 as a γ-glutamylcysteine synthetase highlights the importance of glutathione in disease resistance of Arabidopsis. Plant J **49:** 159–172

Qiu QS, Huber JL, Booker FL, Jain V, Leakey AD, Fiscus EL, Yau PM, Ort DR, Huber SC (2008) Increased protein carbonylation in leaves of Arabidopsis and soybean in response to elevated [CO2]. Photosynth Res **97:** 155–166

Queval G, Neukermans J, Vanderauwera S, Van Breusegem F, Noctor G (2012) Day length is a key regulator of transcriptomic responses to both CO_2 and H_2O_2 in *Arabidopsis*. Plant Cell Environ **35:** 374–387

Queval G, Noctor G (2007) A plate reader method for the measurement of NAD, NADP, glutathione, and ascorbate in tissue extracts: application to redox profiling during Arabidopsis rosette development. Anal Biochem **363:** 58–69

Rius SP, Casati P, Iglesias AA, Gomez-Casati DF (2006) Characterization of an *Arabidopsis thaliana* mutant lacking a cytosolic non-phosphorylating glyceraldehyde-3-phosphate dehydrogenase. Plant Mol Biol **61:** 945–957

Ruiz C, Pla M, Company N, Riudavets J, Nadal A (2016) High CO_2 concentration as an inductor agent to drive production of recombinant phytotoxic antimicrobial peptides in plant biofactories. Plant Mol Biol **90:** 329–343

Siemens J, González MC, Wolf S, Hofmann C, Greiner S, Du Y, Rausch T, Roitsch T, Ludwig-Müller J (2011) Extracellular invertase is involved in the regulation of clubroot disease in *Arabidopsis thaliana*. Mol Plant Pathol **12:** 247–262

Stuttmann J, Hubberten HM, Rietz S, Kaur J, Muskett P, Guerois R, Bednarek P, Hoefgen R, Parker JE (2011) Perturbation of *Arabidopsis* amino acid metabolism causes incompatibility with the adapted biotrophic pathogen *Hyaloperonospora arabidopsidis*. Plant Cell **23:** 2788–2803

Tallis MJ, Lin Y, Rogers A, Zhang J, Street NR, Miglietta F, Karnosky DF, De Angelis P, Calfapietra C, Taylor G (2010) The transcriptome of Populus in elevated CO reveals increased anthocyanin biosynthesis during delayed autumnal senescence. New Phytol **186:** 415–428

Teles CS, Benedetti BC, Gubler WD, Crisosto CH (2014) Prestorage application of high carbon dioxide combined atmosphere storage as a dual approach to control *Botrytis cinerea* in organic 'Flame Seedless' and 'Crimson Seedless' table grapes. Postharvest Biol Technol **89:** 32–39

Tian W, Hou C, Ren Z, Pan Y, Jia J, Zhang H, Bai F, Zhang P, Zhu H, He Y, et al (2015) A molecular pathway for CO_2 response in Arabidopsis guard cells. Nat Commun **6:** 6057

Torres MA, Jones JDG, Dangl JL (2006) Reactive oxygen species signaling in response to pathogens. Plant Physiol **141:** 373–378

Vahisalu T, Kollist H, Wang YF, Nishimura N, Chan WY, Valerio G, Lamminmäki A, Brosché M, Moldau H, Desikan R, et al (2008) SLAC1 is required for plant guard cell S-type anion channel function in stomatal signalling. Nature **452:** 487–491

Vanacker H, Carver TL, Foyer CH (2000) Early H_2O_2 accumulation in mesophyll cells leads to induction of glutathione during the hypersensitive response in the barley-powdery mildew interaction. Plant Physiol **123:** 1289–1300

Vlot AC, Dempsey DA, Klessig DF (2009) Salicylic acid, a multifaceted hormone to combat disease. Annu Rev Phytopathol **47:** 177–206

Vogel MO, Moore M, König K, Pecher P, Alsharafa K, Lee J, Dietz KJ (2014) Fast retrograde signaling in response to high light involves metabolite export, MITOGEN-ACTIVATED PROTEIN KINASE6, and AP2/ERF transcription factors in *Arabidopsis*. Plant Cell **26:** 1151–1165

Voll LM, Zell MB, Engelsdorf T, Saur A, Wheeler MG, Drincovich MF, Weber APM, Maurino VG (2012) Loss of cytosolic NADP-malic enzyme 2 in *Arabidopsis thaliana* is associated with enhanced susceptibility to *Colletotrichum higginsianum*. New Phytol **195:** 189–202

Wildermuth MC, Dewdney J, Wu G, Ausubel FM (2001) Isochorismate synthase is required to synthesize salicylic acid for plant defence. Nature **414:** 562–565

Wilson DC, Carella P, Isaacs M, Cameron RK (2013) The floral transition is not the developmental switch that confers competence for the *Arabidopsis* age-related resistance response to *Pseudomonas syringae* pv. *tomato*. Plant Mol Biol **83:** 235–246

Zhang S, Li X, Sun Z, Shao S, Hu L, Ye M, Zhou Y, Xia X, Yu J, Shi K (2015) Antagonism between phytohormone signalling underlies the variation in disease susceptibility of tomato plants under elevated CO_2. J Exp Bot **66:** 1951–1963